

Nuclear-Magnetic-Resonance Study of Heavily Nitrogen-Doped Silicon Carbide*

MICHAEL N. ALEXANDER†

Laboratory of Atomic and Solid State Physics, Cornell University, Ithaca, New York 14850

(Received 26 February 1968)

Samples of heavily nitrogen-doped silicon carbide (SiC:N) have been studied by use of pulse nuclear magnetic resonance (NMR) at a resonance frequency of 8.5 MHz. Measurements were made, for Si²⁹ and C¹³, of the Knight shift, the spin-lattice relaxation time T_1 , and the free-induction decay time T_2^* (which is inversely proportional to the linewidth). The samples of SiC:N studied had nitrogen donor concentrations n_d estimated to be in the range $1.9 \times 10^{19} \lesssim n_d \lesssim 6.0 \times 10^{20} \text{ cm}^{-3}$. Samples for which $n_d < 10^{20}$ were of the 6H polytype, and samples for which $n_d > 10^{20}$ were of the cubic polytype. The measurements on the cubic SiC:N samples show a markedly different behavior of the electron interaction with the silicon and carbon sublattices. The T_1 's of Si²⁹ are an order of magnitude larger than those of C¹³ for these samples. In no case is the Si²⁹ Knight shift observable, whereas the C¹³ Knight shift increases with n_d , and is $0.9 \pm 0.1 \text{ G}$ (in 7.92 kG) for the most heavily doped sample; the measured C¹³ Knight shifts agree with the C¹³ Knight shifts predicted from T_1 , using the Korringa relation. The C¹³ linewidth increases with n_d , suggesting that the linewidth is determined by a distribution of Knight shifts. From the temperature dependence of both the Si²⁹ and C¹³ T_1 's, it is inferred that the electron system is degenerate in the cubic SiC:N samples. The results can be explained in terms of the electron wave functions appropriate to the conduction-band minimum in cubic SiC. Thus it is inferred that the electron degeneracy in these samples is associated with the Fermi energy lying in the conduction band of the host SiC. The NMR properties of the 6H SiC:N samples are dominated by nuclear interaction with paramagnetic electrons localized, at liquid-helium temperatures, on donor sites or donor complexes. The temperature dependence of T_1 and of the linewidth indicates that electrons are "frozen" on donor sites and donor complexes at liquid-helium temperatures, and are thermally activated at higher temperatures. The results of the NMR study of 6H SiC:N are compared to results from electron-transport measurements; the transport measurements, which were made at temperatures higher than those used in this experiment, indicate that the electron systems of these samples are characterized by the existence of delocalized, mobile electrons.

I. INTRODUCTION

THIS paper reports the investigation, using pulsed nuclear magnetic resonance (NMR), of the resonance properties of Si²⁹ and C¹³ nuclei in heavily nitrogen-doped silicon carbide (SiC:N).¹ We are interested in the properties of samples having nitrogen donor concentrations sufficiently large that strong overlap between donor electron wave functions leads to delocalization of the donor electrons.^{2,3} The research to be described here is thus similar to that on phosphorous-doped silicon (Si:P) reported several years ago by Sundfors and Holcomb.⁴ One of the reasons for undertaking this research, aside from interest in SiC itself, was in fact to learn to what extent the results for Si:P are applicable to heavily doped semiconductors in general, and to see what else might be learned about the "metallic transition" phenomenon. SiC is a system

similar to Si most notably in that Si and C are both group-IV elements and in that the bonding is tetrahedral and primarily covalent; SiC differs from Si in several ways, however. For example, the band gap in SiC is 2.4–3.3 eV (depending on the SiC polytype) as compared to 1.14 eV for Si, and the impurity ionization energies are greater in SiC than in Si.⁵ Some comparisons between SiC:N and Si:P will be made in this article; however, we will focus primarily on SiC:N itself, since a more detailed discussion of SiC:N in relation to Si:P will be made elsewhere.⁶

The experimental research reported here includes measurements of the spin-lattice relaxation time T_1 , the resonance field shift (Knight shift) $K \equiv \Delta H_0/H_0$, the transverse relaxation time T_2^* , and the line shape. T_2^* is the nuclear free-induction decay time; the shape of the free-induction decay is the Fourier transform of the absorption line.⁷

Since this study is concerned with the delocalization of electrons and resultant formation of a degenerate electron system, we briefly review the relevant aspects of NMR for spin- $\frac{1}{2}$ nuclei in a solid having a degenerate electron system.^{8,9} When spin- $\frac{1}{2}$ nuclei interact with a

* This article is based on the Ph.D. thesis of M. N. Alexander, Cornell University, 1967 (unpublished). Research supported by the U.S. Army Research Office, Durham, under Contract No. DA-31-124-ARO-D-407, Technical Report No. 7.

† Present address: Materials Research Laboratory, Army Materials and Mechanics Research Center, Watertown, Mass. 02172.

¹ A preliminary report of some of these results has been given by M. N. Alexander and D. F. Holcomb, *Bull. Am. Phys. Soc.* **12**, 469 (1967). Because of restrictions on the length of abstracts submitted to *Bull. Am. Phys. Soc.*, it was necessary to omit specification, in the preliminary report, of the SiC polytypes studied.

² N. F. Mott and W. D. Twose, *Advan. Phys.* **10**, 107 (1961).

³ N. F. Mott, *Advan. Phys.* **16**, 49 (1967).

⁴ R. K. Sundfors and D. F. Holcomb, *Phys. Rev.* **136**, A810 (1964).

⁵ A. R. Verma and P. Krishna, *Polymorphism and Polytypism in Crystals* (John Wiley & Sons, Inc., New York, 1966).

⁶ D. F. Holcomb and M. N. Alexander, in *Proceedings of the International Conference on Metal-Nonmetal Transition*, San Francisco, 1968 (unpublished); M. N. Alexander and D. F. Holcomb, *Rev. Mod. Phys.* (to be published).

⁷ I. J. Lowe and R. E. Norberg, *Phys. Rev.* **107**, 46 (1957).

⁸ C. P. Slichter, *Principles of Magnetic Resonance* (Harper and Row, New York, 1963), Secs. 4.7 and 5.3.

⁹ A. Abragam, *Principles of Nuclear Magnetism* (Oxford University Press, New York, 1961), Chaps. VI and IX.

degenerate electron system, the most effective nuclear relaxation mechanism often is provided by the Fermi contact term of the hyperfine interaction,

$$\mathfrak{H}C = - (8\pi/3) \gamma_e \gamma_n \hbar \delta(\mathbf{r}) \mathbf{I} \cdot \mathbf{S}, \quad (1)$$

where γ_e and γ_n are the electron and nuclear magnetogyric ratios, respectively, \mathbf{S} and \mathbf{I} are the electron and nuclear spin vectors, and the vector \mathbf{r} in the Dirac δ function is measured from an origin at the nucleus. The nuclear spin-lattice relaxation rate is given by the relation

$$1/T_1 \propto \langle |\psi(0)|^2 \rangle_{E_F} \rho^2(E_F) T, \quad (2)$$

where T is the absolute temperature, $\psi(0)$ is the value of the electron wave function at the nuclear site, the angular brackets denote an average over the Fermi surface, and $\rho(E_F)$ is the electron density of states at the Fermi surface. (The temperature dependence $T_1 T = \text{const}$ holds whenever the electron system is degenerate and does not require the further assumption that the contact interaction is dominant.) The Knight shift obeys the relation

$$K \propto \langle |\psi(0)|^2 \rangle_{E_F} \chi_e^s, \quad (3)$$

where χ_e^s is the electron spin susceptibility. Both K and T_1 thus measure the amplitude of the electron wave function at the nucleus—an important property that will be utilized in the analysis of the experimental results. If the electrons are in a parabolic band,

$$\rho(E_F) \propto n^{1/3},$$

where n is the electron density; hence $T_1 \propto n^{-2/3}$ for a parabolic band. If the electron spin susceptibility is the Pauli susceptibility, then $\chi_e^s \propto \rho(E_F)$; thus, if the band is parabolic, $K \propto n^{1/3}$. Finally, if the contact term is dominant in the relaxation rate and if $\chi_e^s \propto \rho(E_F)$, then the Korringa relation¹⁰

$$K^2 = (1/T_1 T) (\hbar/4\pi k) (\gamma_e/\gamma_n)^2 \quad (4)$$

holds (k is the Boltzmann constant).

The experimental work to be described was performed at low temperatures. This was done partly to obtain a better signal-to-noise ratio (the isotopic abundance of Si²⁹ is 4.7% and that of C¹³ is 1.1%), but was done primarily because of the nature of the investigation itself: (1) The lower the temperature the less important are the thermal effects such as phonon interactions with the electrons; (2) working at low temperatures ensures that any inherent degeneracy of the electron system is not destroyed.¹¹

Silicon carbide is a material which has many different crystal structures, known as polytypes. In all SiC polytypes the silicon-carbon bonding is tetrahedral; the different polytypes differ in the arrangements of the

tetrahedra. Two polytypes were studied in this experiment— $6H$ SiC and cubic SiC (often referred to as β -SiC). The designation $6H$ indicates that the crystal symmetry is hexagonal and that the unit cell contains six formula weights of atoms. Cubic SiC is a zinc-blende structure. These differences in crystal structure of different SiC polytypes have nontrivial effects on electronic structure. The low-temperature exciton energy gap for cubic SiC, for example, is 2.390 eV,¹² whereas the low-temperature exciton energy gap for $6H$ SiC is 3.024 eV.¹³ Other information on polytypism and the properties of SiC polytypes may be found in Ref. 5.

The research we report here is, to our knowledge, the first NMR study of cubic SiC; it is the second study of $6H$ SiC, the first study being measurements by Hardeman¹⁴ on one SiC:N sample, in connection with his electron-nuclear double resonance (ENDOR) experiment.

II. SAMPLES

The samples of SiC:N used in this study were prepared by Dr. P. T. B. Shaffer of the Carborundum Co., Niagara Falls, N. Y. The SiC was grown by reacting high-purity carbon and silicon in a special furnace at 2500°C. Nitrogen doping was accomplished by growing the SiC in a chosen overpressure of nitrogen gas; the most heavily doped sample used in this study was grown in 100 atm of N₂. The SiC received was a fine powder, typical particle diameters being less than 0.2 mm. Available data^{15,16} indicate that this diameter is smaller than the rf skin depth at the frequency of the rf NMR field used in this experiment, 8.5 MHz. The SiC powder was placed in a cylindrical mold; melted paraffin was poured into the mold and allowed to percolate through the powder to form a sample.¹⁷

Because the method of SiC crystal growth produces a powder of SiC,¹⁸ it was not possible to determine nitrogen donor concentrations by high-temperature Hall-coefficient measurements. Reliable quantitative chemical analysis for nitrogen in SiC is, moreover, extremely difficult.¹⁸ Therefore, it was decided to estimate donor concentrations by using a graph given by Lely and Kröger¹⁵ of nitrogen concentration as a function of overpressure of N₂ during crystal growth. The graph

¹² W. J. Choyke, D. R. Hamilton, and L. Patrick, Phys. Rev. **133**, A1163 (1964).

¹³ W. J. Choyke and L. Patrick, Phys. Rev. **127**, 1868 (1962).

¹⁴ G. E. G. Hardeman, J. Phys. Chem. Solids **24**, 1223 (1963).

¹⁵ J. A. Lely and F. A. Kröger, in *Semiconductors and Phosphors: Proceedings of the International Colloquium, 1956, in Garmisch-Partenkirchen*, edited by M. Schön and H. Welker (Interscience Publishers, Inc., New York, 1958), p. 525 ff.

¹⁶ G. A. Slack and R. I. Scace, J. Chem. Phys. **42**, 805 (1965).

¹⁷ Use of paraffin does not lead to spurious C¹³ NMR properties in this experiment. The proton dipolar magnetic field at the carbon site, calculated using the length of the C-H bond, leads to a C¹³ T₂* much shorter than any observed in this experiment. In any case, an experimental check was made by attempting to detect a C¹³ NMR signal in a block of paraffin which was approximately the same size as the SiC samples. Apparently, the first 90° pulse saturated the C¹³ system, for no free-induction decay could be detected.

¹⁸ P. T. B. Shaffer (private communication).

¹⁰ J. Korringa, Physica **16**, 601 (1950).

¹¹ This is of importance in semiconducting systems, as can be seen from the fact that a degenerate free-electron gas of 1×10^{18} electrons/cm³ has a Fermi temperature $T_F \cong 40^\circ\text{K}$, and that $T_F \cong 200^\circ\text{K}$ for 1×10^{19} electrons/cm³.

is based on both Hall measurements and chemical analyses done on samples at the Philips Research Laboratories in the Netherlands, and it shows the nitrogen donor concentration to be (approximately) proportional to the square root of the nitrogen overpressure during crystal growth. Slack and Scace checked the extrapolation of this graph by analyzing a SiC:N sample grown in 35 atm of N_2 for nitrogen content (by vacuum fusion); they found their result to be in reasonable agreement with the extrapolation.¹⁶

[We have recently obtained from a commercial laboratory a chemical analysis for nitrogen in some of our SiC:N samples. We postpone discussion of the chemical analysis until Appendix B, because (1) use of the Lely-Kröger graph enables direct comparison of our samples with samples on which electron transport measurements were made¹⁵; (2) the recent chemical analysis does not affect the basic physics we report here; and (3) this chemical analysis presents as many questions as it does answers.]

A list of the SiC samples used in this study is presented in Table I. The donor concentrations listed in Table I are based on the Lely-Kröger data¹⁵ and are estimated to have approximately $\pm 25\%$ uncertainty.

As can be seen from Table I, the range of N_2 pressure used in crystal growth leads to two types of samples: 6H SiC results from the nitrogen pressure being 1 atm or smaller during crystal growth, whereas cubic SiC results from growing crystals in more than 1 atm of nitrogen. This is consistent with the earlier observation by Slack and Scace¹⁶ that the cubic polytype appears to be more stable at high nitrogen concentrations than the 6H polytype.¹⁹

The polytypes of the samples were determined from x-ray powder photographs. In many of the samples, contributions from more than one polytype appeared on the x-ray photographs. But in all cases the minority

SiC polytypes appeared to be in very small amounts, as evidenced by the faintness of their lines on the x-ray photographs. Faint x-ray lines, due to β -Si₃N₄, also appeared on the photographs for the samples that were predominantly cubic SiC. The presence of minority polytypes and of β -Si₃N₄, however, had no observable effect on the experimental results: the measured relaxation rates $1/T_1$ and $1/T_2^*$ did not appear to be composites of two or more rates (due, for example, to different relaxation rates for different polytypes).

III. EXPERIMENTAL APPARATUS AND TECHNIQUES

An NMR pulse apparatus with gated amplifier and phase coherent detection,²⁰ which has evolved from the one originally designed and constructed by Clark,^{21,22} was used for measurements of T_1 , T_2^* , and K . The external steady magnetic field was provided by a Harvey-Wells 12-in. electromagnet with 3-in. gap and was measured by use of an NMR gaussmeter and frequency counter. In this experiment, only differences in magnetic fields were important. Such differences could be measured to an accuracy of ± 0.05 G. The NMR resonance frequency was 8.5 MHz, with a resulting resonance field of approximately 10 kG for Si²⁹ and 8 kG for C¹³.

T_1 measurements were made in the following way. A burst of 10 or more 90° pulses was used to bring the net nuclear magnetization into the plane perpendicular to the steady magnetic field H_0 (i.e., to saturate the nuclear spin system). The pulses in the burst were spaced t_0 from each other, in such a fashion that $6T_2^* < t_0 \ll T_1$ —a condition easily achieved in this experiment. A 90° pulse was then applied at a time τ after the burst to monitor the recovery of the nuclear magnetization along the H_0 direction. The free-induction decay was displayed on an oscilloscope and was photographed. From the photographs, the amplitude of the free-induction decay as a function of τ was obtained, and T_1 was determined.

T_2^* was also determined from photographs of the free-induction decay following an rf pulse.

T_1 and T_2^* were measured at 1.4 and 4.2°K (and at 77°K for 6H samples) for Si²⁹, and at 1.4 and 4.2°K for C¹³; C¹³ measurements were not made at 77°K because of the poor signal-to-noise ratio.

Knight shifts were measured at 4.2°K at the resonance frequency of 8.5 MHz. For several of the samples, Knight shifts were measured at 1.4°K as well as at 4.2°K; the 1.4°K Knight shift results were identical to the 4.2°K results. Shifts were measured relative to a reference sample of very pure SiC.

Two methods were employed in measuring Knight

TABLE I. Characteristics of SiC:N samples.

Sample No.	Polytype	N_2 Pressure during crystal growth (atm)	Donor concentration n_d (cm^{-3})
N-7	6H	0.1	1.9×10^{19}
N-6	6H	0.5	4.2×10^{19}
N-3	6H	1.0	6.0×10^{19}
297	6H	1.0	6.0×10^{19}
N-5	Cubic	12.5	2.1×10^{20}
N-1	Cubic	25.0	3.0×10^{20}
N-4	Cubic	50.0	4.2×10^{20}
N-2	Cubic	100	6.0×10^{20}

¹⁹ A word of caution, however, may be in order. The conditions of crystal growth seem to have a strong influence on the SiC polytype that emerges. One might, for example, be tempted to conclude from Table I that the 6H polytype is more stable than the cubic polytype when samples are grown in low overpressures of nitrogen. However, Dr. Shaffer has grown cubic SiC under vacuum. See also the discussion of the thermodynamics of polytype formation in Ref. 5.

²⁰ M. N. Alexander, Ph.D. thesis, Cornell University, 1967 (unpublished).

²¹ W. G. Clark, Ph.D. thesis, Cornell University, 1961 (unpublished).

²² R. K. Sundfors, Ph.D. thesis, Cornell University, 1963 (unpublished).

TABLE II. Si²⁹ and C¹³ T_1 at 1.4 and 4.2°K in nitrogen-doped SiC.

Donor concentration (cm ⁻³)	Si ²⁹ T_1 (1.4°K) (min)	Si ²⁹ T_1 (4.2°K) (min)	C ¹³ T_1 (1.4°K) (min)	C ¹³ T_1 (4.2°K) (min)
1.9×10 ¹⁹	3.6±0.3	3.4±0.3	6.3±1.2	4.7±0.6
4.2×10 ¹⁹	5.7±0.5	5.1±0.8	8.7±1.2	5.3±1.0
6.0×10 ¹⁹				
(Sample 297)	13.0±1.0	7.7±1.0	8.9±1.0	4.0±1.0
(Sample N-3)	14.3±1.5	8.1±0.8	10.8±1.8	4.7±1.3
2.1×10 ²⁰	80±8	31±3	6.6±0.6	2.2±0.4
3.0×10 ²⁰	50±4	21±4	5.5±0.5	2.1±0.7
4.2×10 ²⁰	58±6	24±2	4.7±1.0	1.7±0.5
6.0×10 ²⁰	70±7	27±3	4.4±0.5	1.6±0.5

shifts: (I) The resonance fields of both the sample and the reference were determined by taking photographs of free-induction decays at magnetic field values spaced less than 0.1 G apart and by determining which decay had the shape appropriate to the resonance condition $\omega_{rf} = \omega_0$. (II) This method utilizes the fact that in phase-coherent detection a portion of the rf oscillator signal is introduced into the receiver amplifier, mixing with the amplified signal from the receiver coil prior to a detector stage. If the steady magnetic field H_0 is slightly off resonance, then there is a beat between the Larmor frequency and the reference oscillator frequency. The observed pattern is the beat modulated by the free-induction decay, which, for a Lorentzian line, has the form

$$\exp(-t/T_2^*) \cos(2\pi f' t), \quad (5)$$

where f' is the beat frequency. The Knight shift was measured by photographing the free-induction decay of the reference sample and of the sample under study at a fixed magnetic field which was slightly off resonance. Then the difference in beat frequencies $\Delta f'$ was determined from the photographs, and the field shift ΔH computed from $\gamma \Delta H = 2\pi \Delta f'$, where γ is the nuclear magnetogyric ratio. This method is valid for decays of the form of Eq. (5)—i.e., for Lorentzian lines—since the maxima and minima of such decays occur with the same period as for $\cos(2\pi f' t)$; all lines observed in this experiment were Lorentzian.

Both methods (I) and (II) allowed resonance-field shifts ΔH to be determined to within ± 0.1 G. Method (I) was used for some samples, method (II) for others; both methods gave identical results for those samples on which both were tried. In practice method (II) proved to be the more convenient one, since in this experiment T_1 was typically several minutes or longer.

IV. EXPERIMENTAL RESULTS AND INTERPRETATION

As mentioned above, two types of SiC:N samples were studied. Samples for which the nitrogen donor concentration $n_d < 10^{20}$ cm⁻³ were of the 6H polytype;

samples for which $n_d > 10^{20}$ cm⁻³ were of the cubic polytype. The description of the experimental results will therefore be given in two sections, one for each polytype. Most of the graphs and tables will, however, include data from both polytypes, in order to conserve space.

A. Cubic SiC

T_1 data for SiC samples at liquid-helium temperatures are presented in Table II and in Figs. 1 and 2.

Figure 1 shows T_1 for C¹³ in SiC samples at 1.4°K. The $T_1 \sim n_d^{-2/3}$ line in Fig. 1 is, as explained earlier, the theoretical concentration dependence of T_1 for a metal containing free electrons (i.e., for a parabolic band). The line is normalized to the point for the most heavily doped sample because in the analogous case of T_1 in Si:P, data points conform more closely to the line as donor concentration increases.⁴ As can be seen from Table II, $T_1 T$ is constant between 1.4 and 4.2°K for C¹³ in the cubic SiC samples.

The donor concentration dependence of the Si²⁹ T_1 in cubic SiC:N at 1.4°K, shown in Fig. 2, contrasts sharply with that of C¹³. The Si²⁹ T_1 is an order of mag-

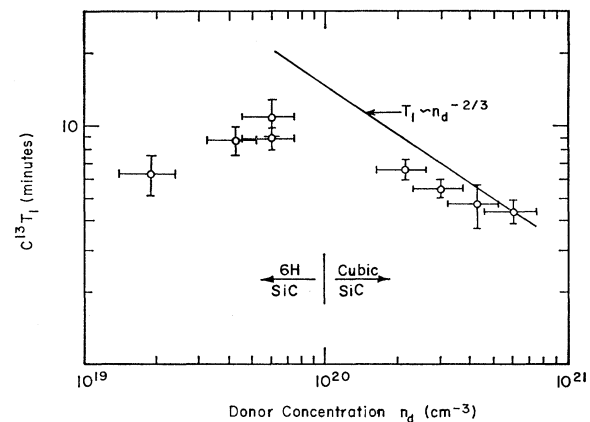


FIG. 1. Donor concentration dependence of C¹³ T_1 in SiC:N at 1.4°K. Samples having donor concentrations smaller than 10^{20} /cm³ are of the 6H polytype, and samples having donor concentrations greater than 10^{20} /cm³ are of the cubic polytype.

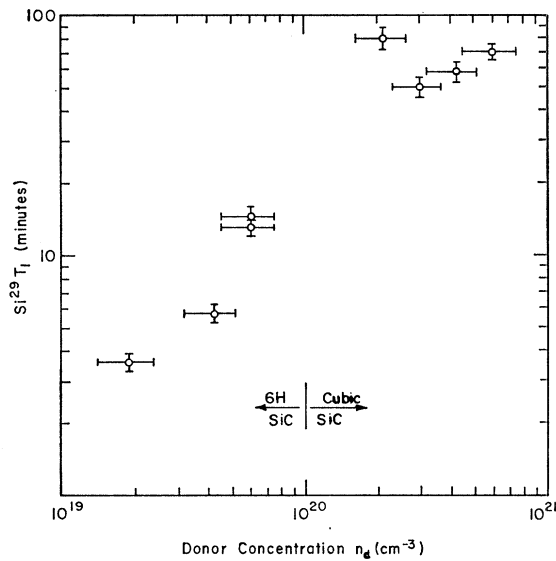


FIG. 2. Donor concentration dependence of $\text{Si}^{29} T_1$ in SiC:N at 1.4°K . Samples having donor concentrations smaller than $10^{20}/\text{cm}^3$ are of the $6H$ polytype, and samples having donor concentrations greater than $10^{20}/\text{cm}^3$ are of the cubic polytype.

nitude larger than the $\text{C}^{13} T_1$ and appears possibly to increase a little with increasing donor concentration. This behavior suggests that the electron system, which, through the contact hyperfine interaction, provides one of the most potent T_1 relaxation mechanisms, is substantially decoupled from the silicon sublattice. (In Fig. 2, sample N-5, with $n_d = 2.1 \times 10^{20}$, has the longest T_1 . This may result from the fact that sample N-5 is freer of unwanted impurities than the other samples, as determined by chemical analysis.¹⁵)

This disparity between the NMR properties of Si^{29} and C^{13} in the cubic SiC:N samples is also apparent in the Knight shift data. In none of the samples was the Si^{29} Knight shift detectable outside the ± 0.1 -G uncertainty in measurement. The C^{13} Knight shift was,

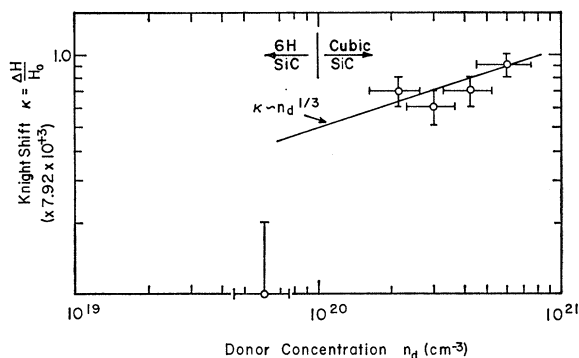


FIG. 3. Donor concentration dependence of C^{13} Knight shift in SiC:N. Samples having donor concentrations smaller than $10^{20}/\text{cm}^3$ are of the $6H$ polytype, and samples having donor concentrations greater than $10^{20}/\text{cm}^3$ are of the cubic polytype. The values on the ordinate are the measured resonance field shifts ΔH , in gauss, at $H_0 = 7.92$ kG.

TABLE III. Comparison of measured and calculated^a Knight shifts for C^{13} in nitrogen-doped SiC (4.2°K).

Donor concentration (cm^{-3})	$K_{\text{meas}}/K_{\text{calc}}$
1.9×10^{19} ($6H$ sample)	≈ 0
4.2×10^{19} ($6H$ sample)	≈ 0
6.0×10^{19} ($6H$ sample)	0.20 ± 0.10
2.1×10^{20} (cubic sample)	1.16 ± 0.25
3.0×10^{20} (cubic sample)	0.83 ± 0.15
4.2×10^{20} (cubic sample)	0.88 ± 0.17
6.0×10^{20} (cubic sample)	1.07 ± 0.10

^a Calculation made by inserting the measured T_1 at 4.2°K in the Korringa relation, Eq. (4).

in contrast to this, detectable, and the results are presented in Fig. 3. As in Fig. 1, the line drawn is the theoretical dependence of K on n_d for a distribution of noninteracting electrons obeying Fermi statistics.

Table III presents the evidence that the C^{13} Knight shifts are correlated with the T_1 's through the Korringa relation, Eq. (4). C^{13} Knight shifts calculated from the T_1 's at 4.2°K are in agreement with the measured Knight shifts. This reinforces the impression that the contact hyperfine interaction is the dominant one for the carbon sublattice in heavily doped cubic SiC and that the electron system is strongly degenerate.

The donor concentration dependence of the C^{13} linewidth is presented in Fig. 4. The linewidth increases with donor concentration, suggesting that the broadening is caused by a distribution of Knight shifts, as was the case for Si:P.⁴ There was no comparable broadening of the Si^{29} line in SiC as a function of donor concentration. Si^{29} linewidths (linewidths were calculated from $\delta H = 1/\gamma T_2^*$ for both C^{13} and Si^{29}) for the cubic SiC samples varied from 0.14 to 0.26 G, exhibiting no trend as a function of n_d ; the lines were so narrow that differences in linewidth between samples could have been due to differences in homogeneity of the static magnetic field in the various data runs.

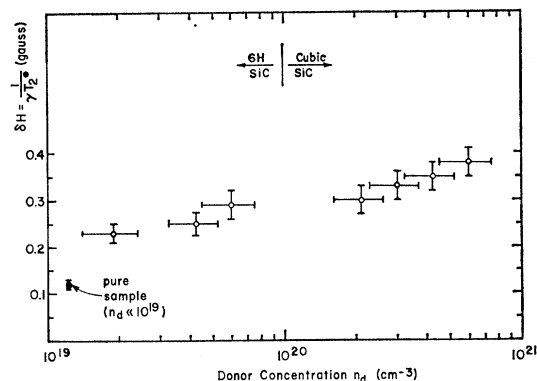


FIG. 4. Donor concentration dependence of C^{13} linewidth in SiC:N at 1.4°K . Samples having donor concentrations smaller than $10^{20}/\text{cm}^3$ are of the $6H$ polytype, and samples having donor concentrations greater than $10^{20}/\text{cm}^3$ are of the cubic polytype.

TABLE IV. Free-induction decay times T_2^* for samples of nitrogen-doped $6H$ SiC. The electromagnet had to be moved between different data runs in this experiment, to allow other experiments to be performed. This led to slight differences in the inhomogeneity in the static magnetic field from one data run to another; the inhomogeneity was 4–7 parts in 10^6 .^a T_2^* data for the two most lightly doped samples were taken during the same data run, and therefore may be compared directly. Because the data for the most heavily doped sample (N-3) were taken during another run, the homogeneity of the static magnetic field is slightly different for this sample; a direct comparison between the T_2^* value for this sample and the values for the other two samples should be treated with care. The relation between T_2^* and the linewidth δH is $\delta H = 1/\gamma T_2^*$, where γ is the nuclear magnetogyric ratio.

n_d (cm^{-3})	Si ²⁹ T_2^* 1.4°K (μsec)	Si ²⁹ T_2^* 4.2°K (μsec)	Si ²⁹ T_2^* 77°K (μsec)	C ¹³ T_2^* 1.4°K (μsec)	C ¹³ T_2^* 4.2°K (μsec)
1.9×10^{19}	770 ± 50	1020 ± 80	1150 ± 200	640 ± 60	690 ± 100
4.2×10^{19}	800 ± 80	960 ± 100	1200 ± 200	600 ± 60	710 ± 80
6.0×10^{19}	740 ± 50	850 ± 50	1150 ± 200	510 ± 50	570 ± 60

^a Reference 20.

Both the Si²⁹ and the C¹³ line shapes were Lorentzian in the cubic SiC:N samples. The linewidths in the cubic samples exhibited no temperature dependence at liquid-helium temperatures.

The discussion for heavily doped cubic SiC:N has, thus far, made two principal points. First, the electrons on the carbon sublattice exhibit “metallic” properties. Second, there is a disparity between the NMR properties of C¹³ and Si²⁹, shown most strikingly by the disparity in the magnitude of their T_1 's.

Some light is thrown on the nature of this disparity by the temperature dependence, at liquid-helium temperatures, of the Si²⁹ T_1 's (Table II). If the long Si²⁹ T_1 's of the samples were due to dipolar interaction with electrons localized on nitrogen donor sites or were due to spin diffusion to paramagnetic impurities, T_1 would be expected to show a weak temperature dependence. But, as can be seen from Table II, the Si²⁹ T_1 's in fact have strong temperature dependences. $T_1 T$ is not constant for Si²⁹ in the cubic samples, but the deviation from $T_1 T = \text{const}$ is only 20–30%. This is a relatively small deviation, considering the length of the relaxation times for these samples; with such long relaxation times, nuclear relaxation by electrons on paramagnetic impurities other than nitrogen might contribute noticeably to the observed T_1 . This temperature dependence suggests that (1) the metallic electrons which are responsible for the C¹³ relaxation properties are also primarily responsible for the Si²⁹ NMR properties of heavily doped SiC:N, and (2) as may be concluded from the lack of an observable Si²⁹ Knight shift and from the long Si²⁹ T_1 values, the wave-function density of these metallic electrons is very small on the Si sublattice in these samples.

These conclusions can be explained in terms of calculated band structures for cubic SiC. Such calculations^{23–25} predict conduction-band minima at the

²³ S. Kobayasi, J. Phys. Soc. Japan **13**, 261 (1958).

²⁴ F. Bassani and M. Yoshimine, Phys. Rev. **130**, 20 (1963); F. Bassani, in *Semiconductors and Semimetals*, edited by R. K. Willardson and A. C. Beer (Academic Press Inc., New York, 1966), Vol. 1, p. 21 ff. (see especially pp. 61–67).

²⁵ F. Herman, R. L. Kortum, and C. D. Kuglin, Intern. J. Quantum Chem. **1S**, 533 (1967); F. Herman (private communication).

Brillouin-zone boundary in the (100) directions (the X point), and optical experimental data¹² support this conclusion. Wilkins has examined the form of the wave functions for the conduction bands at this point.²⁶ He finds that the wave function for the conduction-band minimum, associated with the irreducible representation X_1 ,²⁷ has zero amplitude on silicon sites and maximum amplitude on carbon sites. (Details are presented in Appendix A.)

It is apparent that the properties of this wave function provide a ready explanation for the strikingly different magnitudes of the electron interactions with the Si²⁹ and C¹³ nuclei in the cubic SiC samples. This suggests strongly that, in the cubic SiC samples studied, the Fermi energies of their respective degenerate electron systems lie in the conduction band of the host SiC and that the electrons exhibit properties appropriate to the conduction band of the *host* SiC (rather than, for example, properties appropriate only to an “impurity band”).

This conclusion supports the choice by Bassani and Yoshimine²⁴ and by Herman *et al.*²⁵ of X_1 as the lowest conduction-band level: wave functions for X_3 and X_5 (notation of Ref. 27) are not consistent with the experimental results (see Appendix A).

B. $6H$ SiC

Results for $6H$ SiC are included in Figs. 1–4 and in Tables II and III, discussed above in connection with cubic SiC. Additional results for $6H$ SiC are given in Fig. 5 and in Table IV.

The NMR properties of the $6H$ SiC samples differ from those of the cubic SiC samples in many ways. First, $T_1 T$ is not constant for the $6H$ samples. In fact, for samples N-6 and N-7, the Si²⁹ T_1 is virtually independent of temperature at liquid-helium temperatures (see Table II and Fig. 5).²⁸ Second, both the Si²⁹ and the C¹³ Knight shifts for the $6H$ samples are not meas-

²⁶ J. W. Wilkins (private communication).

²⁷ L. P. Bouckaert, R. Smoluchowski, and E. P. Wigner, Phys. Rev. **50**, 58 (1936).

²⁸ The $T_1 T$, at liquid-helium temperatures, of C¹³ in sample N-3 might possibly be interpreted to be constant; but that interpretation requires liberal use of the measurement uncertainties.

urable outside the 0.1-G measurement uncertainty; the Knight shifts calculated from the T_1 's measured at 4.2°K, using Eq. (4), would, however, definitely be observable (see, e.g., Table III). Third, the NMR linewidths of the 6H samples (all lines were of Lorentzian shape) show a definite temperature dependence, the lines broadening as temperature decreases (Table IV).

The behavior described in the above paragraph is not that characteristic of nuclear interaction with a degenerate electron system. In fact, the weak temperature dependence of the T_1 's and the broadening of the NMR lines as temperature decreases indicate that at low temperatures electrons are being "frozen" onto donor sites or onto complexes of donor sites. For then T_1 at liquid-helium temperatures is determined by fluctuations in the dipole magnetic field due to unpaired localized electrons and by nuclear spin diffusion to the paramagnetic sites²⁹—processes that are expected to have a weak temperature dependence.

The narrowing of the NMR lines as temperature increases may be regarded as a motional narrowing phenomenon: As electrons are thermally excited so that they no longer are localized on donor sites or complexes, the time averages of the electron dipole magnetic fields seen by the Si²⁹ and C¹³ nuclei decrease, and hence their NMR linewidths decrease. A related effect on the electron spin-resonance spectrum in 6H SiC:N has been reported by Hardeman.¹⁴ Hardeman found that in a 6H sample having $n_d = 10^{19}$ (*sic*) the ESR spectrum at 1.2°K shows hyperfine structure appropriate to localized donor electrons, whereas at 77°K there is no hyperfine structure.

The quantitative reasonableness of the model given above may be tested by a simple calculation. The linewidth δH in gauss, due to dilute paramagnetic impurities, is given by

$$\delta H = 3.8\gamma\hbar n, \quad (6)$$

where γ , here, is the magnetogyric ratio of the electron and n is the density of paramagnetic electrons.³⁰ The measured linewidths were $\delta H \approx 0.25$ G; if we use this value of δH in Eq. (6), we find $n \approx 4 \times 10^{18}$. This result is in reasonable agreement with the experimental result of van Wieringen³¹ that in a 6H SiC:N having 1.1×10^{19} donors/cm³ the concentration of paramagnetic impurities (determined from the integrated ESR intensity) was 4×10^{18} /cm³.

We may summarize the interpretation of the NMR results for the 6H SiC:N samples by stating that the liquid-helium temperature NMR properties of the samples are those characteristic of nuclear interaction with electrons bound to individual donor sites or to donor complexes. The temperature dependences of T_1 and T_2^* indicate that at 77°K many of the electrons,

which at liquid-helium temperatures are apparently localized, move over large volumes of the crystal; this is evidenced most strongly by the fact that T_2^* at 77°K is essentially the same as for a pure SiC crystal, in which the linewidth is due to internuclear dipole interactions. The fact that the T_1 's of samples 297 and N-3 exhibit a markedly stronger temperature dependence between 1.4 and 4.2°K than do the T_1 's of the less heavily doped 6H samples indicates that the electrons in samples 297 and N-3 are less localized than in the other samples; this interpretation is supported by the T_2^* data, which show the linewidth of sample N-3 to have the weakest temperature dependence of the 6H samples at liquid-helium temperatures.

Lely and Kröger¹⁵ and Violina *et al.*³² have measured the electrical resistivity and the Hall coefficient of 6H SiC:N samples for temperatures $T > 90^\circ\text{K}$. They have found that, for samples in which $n_d \gtrsim 2 \times 10^{19}$ cm⁻³, both the Hall coefficient and the resistivity are independent of temperature over a large range of temperature. The inference drawn from the data was that since the density of carriers is constant over a large range of temperature, the electrons are delocalized. (Definite temperature dependences are observed for the Hall coefficient and for resistivity for $n_d < 2 \times 10^{19}$; thus it appears from the transport data that a "metallic transition" occurs, for 6H SiC:N, at $n_d \approx 2 \times 10^{19}$.)

This conclusion would seem to be in conflict with conclusions that might be drawn from the NMR data. It is somewhat difficult to compare the two sets of data, in attempting to resolve the apparent conflict, because the electron transport data were obtained at higher temperatures than the temperatures at which this NMR experiment was performed. If there is a temperature dependence, for $T < 90^\circ\text{K}$, in the Hall coefficient and resistivity, it may correlate in a straightforward way with our NMR measurements. However, since the electron transport data for $T > 90^\circ\text{K}$ contain no hint that measurements for $T < 90^\circ\text{K}$ might reveal temperature dependences in electron transport data, we have no right to *assume* at this time that such a temperature dependence exists. We will therefore continue the inquiry into this apparent conflict between the NMR and electron transport data, assuming that there is no temperature dependence of the Hall coefficient and resistivity, even at low temperatures.

Important differences in donor concentration between our samples and those used in the transport measurements are unlikely, especially since the donor concentrations assigned to samples used in this study were based on a graph which Lely and Kröger themselves had made (samples they used in electron transport measurements were among those which provided the data used in constructing the graph). Chemical analyses^{18,33} show that compensation is not important in our samples.

²⁹ Reference 9, pp. 378–389.

³⁰ Reference 9, Chap. IV, Sec. IV B.

³¹ J. S. van Wieringen, in Ref. 15, p. 367 ff.

³² G. N. Violina, Yeh Liang-hsiu, and G. F. Kholuyanov, *Fiz. Tverd. Tela* 5, 3406 (1963) [English transl.: *Soviet Phys.—Solid State* 5, 2500 (1964)].

³³ R. K. Skogerboe (private communication).

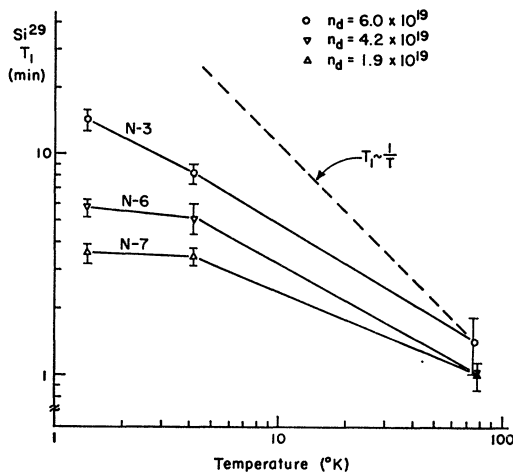


FIG. 5. Si^{29} T_1 as function of temperature for $6H$ SiC:N samples.

It is possible that what has, at first sight, seemed to be a discrepancy between the NMR and the electron transport measurements may not be a real discrepancy at all. We have noted that the NMR properties of the $6H$ SiC:N samples are those characteristic of nuclear interaction with localized electrons. However, we have, been careful not to jump to the conclusion that the electron systems of the samples are characterized *completely* by localized electrons, especially since the rough estimate made above showed that the NMR properties can be accounted for by nuclear interaction with only $\approx 4 \times 10^{18}$ donor electrons/cm³ in a total of $2\text{--}6 \times 10^{19}$ donor electrons/cm³. It might therefore be the case that the interpretations of both the NMR and the electron transport measurements are simultaneously correct—that a “metallic transition” does occur in $6H$ SiC:N at a donor concentration $n_d \approx 2 \times 10^{19}$ cm⁻³ (as indicated by the electron transport measurements), but that even above the “transition” concentration there is a small but nonetheless significant concentration of localized electrons (as indicated by the NMR measurements).

If most of the electrons are delocalized, the Hall coefficient and resistivity should be fairly insensitive to the presence of a relatively small concentration of localized electrons. On the other hand, NMR can be more sensitive than the transport measurements to the presence of a small percentage of localized paramagnetic electrons, particularly if this small percentage is greater than 10^{18} /cm³. The contribution of the localized electrons to the nuclear spin-lattice relaxation rate might be of the same order of magnitude as, or even exceed, the contribution due to delocalized electrons. In the case of the $6H$ SiC:N samples, it follows from the interpretation of the data given in the last paragraph that the nuclear interaction with the localized electrons dominates that with the delocalized electrons. This is quite plausible. The T_1 data of Fig. 5, for ex-

ample, can be interpreted in this light in the following way: If T_1 at 77°K is taken to be the lower limit for T_1 due only to delocalized electrons (it is a lower limit because there may be some localized electrons present and contributing to the observed T_1), then from $T_1 T = \text{const}$ the relaxation time at liquid-helium temperatures due to the delocalized electrons is much longer than that which is actually observed.

V. SUMMARY

Samples of heavily nitrogen-doped SiC have been studied, using pulse NMR at a resonance frequency of 8.5 MHz. Measurements were made, for Si^{29} and C^{13} , of the Knight shift, the spin-lattice relaxation time T_1 , and the free-induction decay time T_2^* (which is inversely proportional to the linewidth). Samples of the $6H$ polytype and of the cubic polytype were studied.

The measurements on the cubic SiC:N samples show a markedly different behavior of the electron interaction with the silicon and carbon sublattices. Si^{29} T_1 's are an order of magnitude larger than the C^{13} T_1 's. In no case is the Si^{29} Knight shift observable outside the experimental error of ± 0.1 G, whereas the C^{13} Knight shift is observable and increases with donor concentration. The measured C^{13} Knight shifts agree with the C^{13} Knight shifts predicted from T_1 , using the Korringa relation. The C^{13} linewidth increases with donor concentration in a fashion which suggests that the linewidth is determined by a distribution of Knight shifts.

From the temperature dependence of both the Si^{29} and C^{13} T_1 's it is inferred that the electron system is degenerate in the cubic SiC:N samples. The results can be explained in terms of the band structure of cubic SiC, since the wave function appropriate to the conduction-band minimum in cubic SiC has maximum amplitude on carbon sites and zero amplitude on silicon sites. Thus it is inferred that the degenerate electron system in the cubic SiC:N samples studied has its Fermi energy lying in the conduction band of the host SiC and that the electrons exhibit properties appropriate to the host system.

The NMR properties of the $6H$ SiC:N samples appear to be dominated by nuclear interaction with paramagnetic electrons localized, at liquid-helium temperatures, on donor sites or donor complexes. The Si^{29} and C^{13} T_1 's show a weak temperature dependence. The linewidth decreases as temperature increases; the Si^{29} linewidth at 77°K is approximately the same as that for a sample of pure SiC, in which the linewidth is determined by internuclear dipole interactions. This temperature dependence indicates that electrons are frozen onto donor sites and donor complexes at liquid-helium temperatures.

Published data on electrical resistivity and Hall coefficient data, which were taken at temperatures higher than those used in this experiment, indicate that

the 6H SiC:N samples studied in this experiment have free electrons. The relation of this result to the NMR results of this study has been discussed, and it has been found that the NMR and electron transport results are not necessarily inconsistent.

ACKNOWLEDGMENTS

The author wishes to express his great appreciation for the assistance given by Professor Donald F. Holcomb, who originally suggested this project, and in whose laboratory at Cornell University this research was performed. His criticism of the research was always constructive, and his advice was invaluable at all stages of this work.

Helpful discussions on various aspects of this work were held with Professor J. W. Wilkins, Professor N. W. Ashcroft, Dr. J. A. Kaeck, and G. P. Carver at Cornell University. Professor Wilkins, in particular, was helpful in the interpretation of the NMR results for cubic SiC.

Dr. P. T. B. Shaffer of the Carborundum Co. generously provided the SiC samples and was very helpful in all matters related to sample preparation and analysis. Dr. R. K. Skogerboe of the Analytical Laboratory, Materials Science Center, Cornell University, provided determinations of impurities for some SiC samples. Other Central Facilities of the Center also provided assistance. Dr. F. Herman of Lockheed Palo Alto Research Laboratory made helpful comments concerning band-structure calculations for SiC and furnished the author with a report of his work on cubic SiC.

APPENDIX A: WAVE FUNCTION FOR THE CONDUCTION-BAND MINIMUM IN CUBIC SILICON CARBIDE

Calculations of the band structure of cubic SiC²³⁻²⁵ predict conduction-band minima at the Brillouin-zone boundary in the (100) directions in k space. This prediction has been supported experimentally by the optical work of Choyke *et al.*¹² Since the conduction-band minimum occurs at a symmetry point, wave functions compatible with the band minimum must have the appropriate symmetry; the calculation presented in this Appendix, made by Wilkins,²⁶ exploits these symmetry conditions.

We begin by choosing basis vectors for the Si and C atoms. The carbon atoms are placed at

$$[000], \frac{1}{2}a[101], \frac{1}{2}a[011], \dots,$$

where a is the lattice constant. (Brackets designate vectors in direct space, and parentheses designate vectors in reciprocal space.) Thus Si atoms occur at points obtained by adding the vector

$$\frac{1}{4}a[111]$$

to the positions of the carbon atoms.

First, consider the "empty lattice" states (the states determined by crystal symmetry, but which do not include the effect of the crystal potential) for the point X in reciprocal space where the conduction-band minimum occurs. There are two degenerate "empty lattice" states of lowest energy, corresponding to $k^2=1$; these are labelled X_1 and X_3 .²⁷ The next "empty lattice" energy level is associated with the $(100) + (\bar{1}11) = (011)$ directions, for which $k^2=2$; this level is fourfold degenerate, having states corresponding to the irreducible representations X_1 and X_3 , and two states corresponding to the irreducible representation labelled X_5 .²⁷

The basis functions for these representations are

$$\begin{aligned}\psi_{X_1} &= 2 \cos(2\pi y/a) \cos(2\pi z/a), \\ \psi_{X_3} &= 2 \sin(2\pi y/a) \sin(2\pi z/a), \\ \psi_{X_5} &= i\sqrt{2} \sin[2\pi(y+z)/a] \\ &= i\sqrt{2} \sin[2\pi(y-z)/a],\end{aligned}$$

where x, y, z are Cartesian coordinates in direct space. Crystal symmetry dictates that even when the effects of crystal potential are accounted for, spatial dependences of the wave functions for the special symmetry points must be as above.

We now ask which of the irreducible representations is associated with the conduction-band minimum, when the effect of the crystal potential is accounted for, thus lifting some of the degeneracies. The spatial dependence of ψ_{X_1} is such that there is zero wave-function amplitude on silicon sites and maximum amplitude on carbon sites. ψ_{X_3} has a spatial dependence such that there is maximum amplitude on silicon sites and zero amplitude on carbon sites. ψ_{X_5} concentrates the electron probability density in the regions between the silicon and carbon sites.

Bassani and Yoshimine²⁴ and Herman *et al.*,²⁵ using the same definitions as presented here (origin at C atom, same notations for X_1 and X_3), found in their calculations that X_1 is the bottom of the conduction band. This is in agreement with the fact that ψ_{X_1} is the only one of the wave functions which is consistent with our NMR results (see text) for cubic SiC:N, and this is the basis of our conclusion that in our cubic SiC:N samples the Fermi level is in the conduction band of the host SiC. An earlier calculation by Kobayasi²³ gives X_3 as the conduction-band minimum. This at first sight appears to be inconsistent with our results, but the "inconsistency" may be merely notational: If the origin is taken at the Si atom instead of at the C atom, then in the equations above the roles of ψ_{X_1} and ψ_{X_3} are interchanged, ψ_{X_3} becoming the wave function which concentrates the electrons on the carbon sublattice. The choice of origin was not stated by Kobayasi.²³

The following simple physical interpretation may be made of the above results. Since ψ_{X_5} concentrates the electrons between the atoms, it may be regarded

as describing the Si-C bonding orbitals; therefore X_5 is the topmost valence-band state of X_1 , X_3 , and X_5 , a conclusion supported by the calculations of Refs. 24 and 25. The conduction-band wave functions ψ_{X_1} and ψ_{X_3} are related to the antibonding orbitals (they are not quite the same as the antibonding orbitals themselves, since the symmetry here is that of the entire crystal and not that of an isolated molecule). A qualitative interpretation²⁴ of the fact that X_3 lies above X_1 in energy can be made on the basis of the fact that the atomic energy levels of C are lower than those of Si for their outermost electrons, so that C is more electronegative than Si; thus electrons tend to concentrate in the vicinity of the C atoms rather than in the vicinity of the Si atoms, a situation which is described by the wave function ψ_{X_1} .

APPENDIX B: NITROGEN CONCENTRATION IN SILICON CARBIDE SAMPLES

The nitrogen donor concentrations quoted in the main text were obtained by use of a graph by Lely and Kröger¹⁵ of nitrogen concentration as a function of overpressure of N_2 during crystal growth. The graph was used because it has received some independent support from measurements by Slack and Scace,¹⁶ and because it enables direct comparison of our 6H SiC:N samples with those used by Lely and Kröger for electron transport measurements (see text for details).

We have recently obtained from a commercial laboratory—Ledoux and Co., Teaneck, N. J.—a chemical analysis for nitrogen in some of our SiC:N samples. According to Ledoux, in their method the samples are decomposed by acid attack, followed by distillation of NH_4^+ and titration with standard acid. We understand that the acid attack is at high temperature and that details of the technique will be made public at some future time.^{33,34} The nitrogen concentrations (in cm^{-3})³⁵

for the samples analyzed are as follows: N-7 (0.1 atm): 5.2×10^{19} ; N-3 (1 atm): 5.9×10^{19} ; N-5 ($12\frac{1}{2}$ atm): 4.8×10^{19} ; N-1 (25 atm): 5.5×10^{19} ; N-2 (100 atm): 8.5×10^{19} .

These concentrations are not at all in agreement with those obtained from the Lely-Kröger graph (cf. Table I).³⁶ The nitrogen concentration, as determined by Ledoux, does not go as the square of the pressure of N_2 during crystal growth. In fact, the nitrogen concentration as determined by Ledoux is not even monotonic with the pressure (however, if we restrict our attention to one given polytype, the donor concentration is monotonic with the pressure).

The effect of the Ledoux data—if it is to be accepted—on our results is rather small. The effect on Fig. 1 is to make T_1 follow the $n_d^{-2/3}$ line more closely, while the effect on Fig. 3 is to make the fit of $K \sim n_d^{1/3}$ poorer. The principal effect of the Ledoux data would be to change the donor concentrations to which we attribute the phenomena reported here; while that is not a trivial matter,³⁷ it nevertheless does not affect the basic underlying physics of this investigation—for example, the effects of band structure on the cubic SiC:N data, and the apparent discrepancy between the NMR and electron transport data on what should be essentially similar 6H SiC:N samples.

We are reporting this Ledoux analysis primarily for the sake of completeness. For several reasons—among them the ones mentioned in this Appendix and its footnotes—we are skeptical about these Ledoux analytical results.

³⁶ We recall that Slack and Scace (Ref. 16) checked the extrapolation of the graph at 35 atm N_2 overpressure during crystal growth. In this connection it is worth pointing out that if there is a systematic error in vacuum fusion analysis (the technique Slack and Scace used to determine donor concentration), it would almost certainly be such as to make the measured donor concentration systematically *smaller* than the true donor concentration. Since the Ledoux results give concentrations smaller than those quoted by Slack and Scace, it is all the more difficult to reconcile the two sets of data.

³⁷ The values of T_1 for 6H SiC:N would, if the Ledoux concentrations were used, show extremely sharp increases as a function of donor concentration (especially for Si²⁹). The sharpness of the increases might engender skepticism about the results of the chemical analyses.

³⁴ Conversation between S. Kallman of Ledoux and Co. and R. K. Skogerboe.

³⁵ Concentrations stated by Ledoux were in weight percent; they were converted to cm^{-3} by use of data in P. T. B. Shaffer, *High Temperature Materials* (Plenum Press, Inc., New York, 1964).